

# The High-Redshift Neutral Hydrogen Signature of an Anisotropic Matter Power Spectrum

Oscar F. Hernandez<sup>2,1</sup> and Gilbert P. Holder<sup>1</sup>

<sup>1</sup>*Physics Department, McGill University, 3600 rue University, Montreal, Quebec, Canada H3A 2T8 and*

<sup>2</sup>*Marianopolis College, 4873 Westmount Ave, Westmount, Quebec Canada H3Y 1X9*

An anisotropic power spectrum will have a clear signature in the 21cm radiation from high-redshift hydrogen. We calculate the expected power spectrum of the intensity fluctuations in neutral hydrogen from before the epoch of reionization, and predict the accuracy to which future experiments could constrain a quadrupole anisotropy in the power spectrum. We find that the Square Kilometer Array will have marginal detection abilities for this signal at  $z \sim 17$  if the process of reionization has not yet started; reionization could enhance the detectability substantially. Pushing to higher redshifts and higher sensitivity will allow highly precise (percent level) measurements of anisotropy.

## I. INTRODUCTION

Modern cosmology assumes that the universe is both homogeneous and isotropic when averaged on scales larger than 100 Mpc. Observations, in particular that of the cosmic microwave background (CMB), have established homogeneity and isotropy as valid assumptions if we interpret them statistically. Put another way, “the density of matter may differ from one point in the Universe to another, but the distribution of matter is described as a realization of a random field with a variance that is everywhere the same and the same in every direction” [1]. With the accumulating precision in the measurement of the CMB temperature field and the soon expected polarization data from the Planck satellite, these assumptions can be tested. Ackerman, Carroll and Wise [2] have considered the possibility that rotational invariance was broken in a scale invariant way during inflation, by an effect that has since disappeared. Their paper suggests a possible explanation for hints of anomalies in recent CMB measurements, many of which are carefully discussed, and dismissed as statistical fluctuations in a recent analysis by the WMAP team [3]. Such a preferred direction would be an important clue to the physics of the early universe. Pullen and Kamionkowski [1] have developed CMB power spectrum statistics to detect a direction dependence in the fluctuations in temperature or polarization. Groeneboom et al. [4] have revisited the model of Ackerman et al. to include polarization and various systematic effects.

While the CMB has been a tremendous resource for exploring the physics of the early universe, we are approaching the limits of the information that is encoded: the temperature fluctuations measurements expected from the Planck satellite [5] will be primarily limited by cosmic variance (limits on our ability to characterize variances due to the finite number of independent and informative measurements we can make) in the entire regime where the primary CMB fluctuations are largely unconfused by astrophysical foregrounds. Comparable measurements in polarization would not add a tremendous amount of new information, with the important exception of a possible detection of the signature of gravitational radiation generated in the early universe.

Measurements of large scale structure can in principle provide much more information about the potential fluctuations; the CMB is largely a two dimensional surface, while surveys can probe the three dimensional structure of the universe. Pullen and Hirata [6] have used luminous red galaxies in the Sloan Digital Sky Survey to put the strongest limits on any possible anisotropy, constraining any possible quadrupole anisotropy in the power spectrum to be less than 40%.

On large scales, the fluctuations are small enough such that they are expected to evolve according to linear theory, but small scales are highly non-linear and difficult to model. The scale at which this transition occurs defines the smallest scale which can be readily used for measuring cosmological parameters, which places limits on the number of independent modes of the fluctuations which can be measured. As structure grows in the universe, this scale progressively moves to larger scales. To explore a large number of modes, it is therefore helpful to make measurements at high redshift.

A promising technique for measuring the three-dimensional structure of the universe at high redshift is to measure the 21cm hyperfine transition of neutral hydrogen. In this paper, we investigate the signature of a preferred axis for the fluctuation power in this redshifted 21cm emission.

Neutral hydrogen is the dominant form of baryonic matter in the “dark ages”, i.e. before star formation, hence we expect redshifted 21cm radiation to reach us from all directions in the sky. The intensity of this radiation tells us about the distribution of neutral hydrogen in the universe, as a function of both angular coordinates in the sky and redshift. Thus, in contrast to the CMB, 21cm surveys can probe the three-dimensional distribution of matter in the universe (see [7] for an in-depth review).

As a benchmark experiment, we assume that it will be possible to make arcminute scale measurements with mK sensitivity in a bandwidth of order 1 MHz. This is a somewhat optimistic forecast, but not far beyond what is projected for the Square Kilometer Array [8]. It is expected that  $\sim 250$  square degrees could be surveyed down to frequencies of 70 MHz to a sensitivity of 10 mK, with thousands of frequency resolution elements in a band. At these frequency and spatial resolutions, the smallest accessible scales will be of order a few comoving Mpc. We also consider the benefits of a next generation experiment, an idealized version of an Omniscope [18], that can operate at slightly lower frequencies (to push to higher redshifts), but has a wide field of view. This is a challenging experiment, as the noise rises steeply with lower frequency, but requires only a modest expansion in frequency coverage and a feasible increase in sensitivity.

In what follows below we focus on the signal from before reionization. This simplifies the analysis and is robust to the details of how the first stars formed, but is neglecting a possibly large signal [9]. The 21cm spin temperature during reionization could be substantially different from the CMB temperature in the presence of a UV background, providing a substantial amount of statistical power [10], especially at the lower range of redshifts we consider,  $z \sim 17$ . The details of reionization are sufficiently uncertain at this point that it is difficult to predict the utility of this epoch for precise measurements of the matter power spectrum. It is possible that coupling to Ly- $\alpha$  photons has already coupled the 21-cm spin temperature to the gas temperature at  $z \sim 17$ , but there are currently no observational constraints on this epoch, and there is no exhaustive theoretical search of parameter space that has determined the most likely physical conditions at  $z \sim 17$ . In the sense of signal-to-noise, this would be a large boost over what is assumed in what follows, but it comes at the cost of increased astrophysical uncertainty.

## II. THE 21 CM BRIGHTNESS TEMPERATURE AND ITS POWER SPECTRUM

We can consider the equation of radiative transfer along the line of sight through a hydrogen gas cloud and then compare the intensity of the 21 cm coming through the cloud to a hypothetical ‘‘clear view’’ of the 21 cm radiation from the CMB radiation. This difference in intensity is expressed through the brightness temperature [7] :

$$\delta T_b(z) = \left[ \frac{9c^3 A_{10} \hbar (1-Y)}{128\pi G \nu_{21}^2 k_B m_H H_0 \Omega_m^{1/2}} \right] \left[ \frac{x_{HI}(z)(1+\delta_b(z))(1+z)^{1/2}}{1 + \frac{\partial v_\chi^{pec}/\partial \chi}{H(z)/(1+z)} + \frac{v_\chi^{pec}}{c}} \right] \left[ 1 - \frac{T_\gamma(z)}{T_S} \right] \quad (1)$$

$$= [8.8 \text{ mK}] \left[ \frac{x_{HI}(z)(1+\delta_b(z))(1+z)^{1/2}}{1 + \frac{\partial v_\chi^{pec}/\partial \chi}{H(z)/(1+z)} + \frac{v_\chi^{pec}}{c}} \right] \left[ 1 - \frac{T_\gamma(z)}{T_S} \right] \quad (2)$$

where we have taken the values  $A_{10} = 2.85 \times 10^{-15} \text{ s}^{-1}$ ,  $H_0 = 73 \text{ km s}^{-1} \text{ Mpc}^{-1}$ ,  $\nu_{21} = 1420 \text{ MHz}$ ,  $\Omega_b = 0.0425$ ,  $\Omega_m = 0.26$ .

The brightness temperature in eq. 1 is a function of redshift for a chosen line of sight. Since redshift can be related to the radial distance, we can think of the brightness temperature as a function of  $\vec{x}$ . Redshift  $z$  is related to the comoving radial coordinate  $\chi$  through

$$\chi = \frac{c}{a_0} \int_{\frac{a_e}{a_0}}^1 \frac{da}{a^2 H(a_0 a)} \quad , \quad \frac{a_e}{a_0} = \frac{(1 + v_\chi^{pec}/c)}{(1+z)} \quad (3)$$

For  $1 < z < 3000$  we have a matter dominated universe with  $H(a) = H_0 \sqrt{\Omega_m/a^3}$ . Here and throughout, we assume that the peculiar velocities are non-relativistic.

After recombination Compton heating through the residual free electrons keep the kinetic cosmic gas temperature  $T_K$  and the spin temperature  $T_S$ , equal to the CMB temperature  $T_\gamma$ . As illustrated in ref. [7] fig. 6, the cosmic gas begins to decouple from the CMB at around  $z \sim 300$ . At this point the cosmic gas is dense enough that the spin temperature  $T_S$  is cooled from the CMB temperature to the kinetic cosmic gas temperature  $T_K$  by collisions. By  $z \sim 100$  the cosmic gas begins cooling adiabatically as  $T_K = 0.02 \text{ K}(1+z)^2$ . As the cosmic gas expands collisions between hydrogen atoms become less efficient at cooling the spin temperature. Photon interactions then slow the cooling of the spin temperature, and it is eventually again driven towards the CMB temperature. By the time reionization begins at around redshifts of 20,  $T_S \sim T_\gamma$ , making the 21cm signal relatively small. In this our analysis we are particularly interested in redshifts  $z$ , with  $15 \leq z \leq 35$  when  $T_S \lesssim T_\gamma$ .

We now consider fluctuations in the 21 cm brightness temperature by defining an average of  $\delta T_b$  over all angular coordinates and defining  $\delta_{21}(\vec{x})$  through

$$\delta T_b(\vec{x}) \equiv \overline{\delta T_b}(z)(1 + \delta_{21}(\vec{x})) \quad (4)$$

Fluctuation in the brightness temperature arise through fluctuations in the baryon density  $\delta_b$ , the neutral fraction  $\delta_{x_{HI}}$ , fluctuations in the spin temperature  $\delta_{T_s}$ , and the line of sight peculiar velocity gradient  $\delta_{\partial v}$ .

We are interested in  $z$  much after recombination but before reionization. During this time the neutral fraction fluctuations are so small that we can just take  $x_{HI} = 1$ .

The fluctuations in spin temperature can be related to fluctuations in the CMB temperature  $\delta_{T_\gamma}$ , the cosmic gas kinetic temperature  $\delta_{T_K}$  and the baryonic density fluctuations  $\delta_b$ . This is because the spin temperature is determined solely by the temperatures  $T_\gamma$  and  $T_K$  as long as UV scattering is negligible, which is true before reionization. The relationship between spin and kinetic gas temperatures is expressed through the collision coefficients  $x_c$  which describe the rate of scattering among hydrogen atoms and electrons [11, 12]:

$$\left(1 - \frac{T_\gamma(z)}{T_S}\right) = \frac{x_c}{1+x_c} \left(1 - \frac{T_\gamma(z)}{T_K}\right), \quad x_c = x_c^{eH} + x_c^{HH}, \quad x_c^i = \frac{n^i \kappa_{10}^{iH} T_\star}{A_{10} T_\gamma}. \quad (5)$$

where  $k_B T_\star \equiv \hbar 2\pi \nu_{21} = 0.0682$  K. Fluctuation in the CMB temperature are so small that they can be ignored.

Combining the remaining contributions to  $\delta_{21}$  we calculate that at linear order

$$\delta_{21}(\vec{x}) = \beta_b(z) \delta_b(\vec{x}) + \beta_{T_K}(z) \delta_{T_K}(\vec{x}) - \delta_{\partial v}(\vec{x}), \quad (6)$$

The coefficients  $\beta_b$  and  $\beta_{T_K}$  are

$$\beta_b(z) = 1 + \frac{1}{1+x_c}, \quad (7)$$

$$\beta_{T_K}(z) = \frac{T_\gamma}{T_K - T_\gamma} + \frac{1}{x_c(1+x_c)} \left( x_c^{eH} \frac{\partial \ln \kappa_{10}^{eH}}{\partial \ln T_K} + x_c^{HH} \frac{\partial \ln \kappa_{10}^{HH}}{\partial \ln T_K} \right), \quad (8)$$

Now  $\delta_{T_K}$  is related to  $\delta_b$  via a proportionality constant that depends only on the redshift distance [13]:  $\delta_{T_K}(\vec{x}) = g(z) \delta_b(\vec{x})$ . Fig. 2 in ref. [13] gives the proportionality constant  $g(z)$  for redshift  $z$  between 10 and 1000. We define

$$\beta(z) \equiv \beta_b(z) + g(z) \beta_{T_K}(z) \quad (9)$$

and hence  $\delta_{21}$  in eq. 6 becomes

$$\delta_{21}(\vec{x}) = \beta(z) \delta_b(\vec{x}) - \delta_{\partial v}(\vec{x}) \quad (10)$$

For  $15 < z < 35$ ,  $\beta(z)$  is approximately 1.6 to within 3.5% accuracy.

The line of sight peculiar velocity gradient

$$\delta_{\partial v} \equiv \frac{\partial v_\chi^{pec} / \partial \chi}{H(z)/(1+z)} + \frac{v_\chi^{pec}}{c} \quad (11)$$

introduce redshift space distortions. For scales large enough for linear theory to hold, Kaiser [14] has shown that  $\tilde{\delta}_{\partial v}(\vec{k}) = -f(\hat{k} \cdot \hat{r}_s)^2 \tilde{\delta}_{matter}(\vec{k})$ . Lahav et al. [15] explain that  $f(z) = [\Omega_m(1+z)^3 (H_0/H(z))^2]^{0.6}$  which is essentially unity for the matter dominated universe at the redshifts we are considering. Furthermore we assume that  $\tilde{\delta}_b$  follows  $\tilde{\delta}_{matter}$  for the scales we are considering so that

$$\tilde{\delta}_{\partial v}(\vec{k}) = -(\hat{k} \cdot \hat{r}_s)^2 \tilde{\delta}_b(\vec{k}) \quad (12)$$

We define the power spectra via

$$\langle \tilde{\delta}_{21}(\vec{k}) \tilde{\delta}_{21}(\vec{k}') \rangle \equiv (2\pi)^3 \delta_D^{(3)}(\vec{k} + \vec{k}') P_{21}(\vec{k}), \quad (13)$$

$$\langle \tilde{\delta}_b(\vec{k}) \tilde{\delta}_b(\vec{k}') \rangle \equiv (2\pi)^3 \delta_D^{(3)}(\vec{k} + \vec{k}') P_b(\vec{k}), \quad (14)$$

By writing a spherical harmonic expansion of the 21 cm fluctuations,  $\delta_{21}(\vec{x}) \equiv \delta_{21}(\chi, \hat{x}) = \sum_{l,m} a_{lm}(\chi) Y_{lm}(\hat{x})$  we can construct the angular power spectrum

$$\langle a_{lm}(\chi) a_{l'm'}^\dagger(\chi') \rangle = (4\pi)^2 i^{(l-l')} \int \frac{d^3 k}{(2\pi)^3} j_l(k\chi) j_{l'}(k\chi') Y_{lm}^*(\hat{k}) Y_{l'm'}(\hat{k}) P_{21}(\vec{k}) \quad (15)$$

### III. THE ANGULAR POWER SPECTRUM IN THE FLAT SKY DISTANT OBSERVER APPROXIMATION

We now calculate the 21 cm angular power spectrum in the flat sky approximation distant observer approximation. We look at a tile of sky at the north pole (in the  $\hat{z}$  direction), at an average distance  $\chi_0$ , thickness  $\Delta\chi$ , and angular size  $\Delta\epsilon \times \Delta\epsilon$ . The tile is not too thick, so that the constants in redshift  $z$ , such as  $g(z)$  and  $\beta(z)$  do not vary much and we can treat them as constants. In particular from now on we drop the  $z$  dependence and write simply  $\beta$ . As discussed in the previous section, for the redshifts of interest in this paper  $\beta \approx 1.6$ . We mask the  $\delta(\vec{x})$  so that it is non zero only on that tile. This permits us to extend our integrals beyond the tile's dimensions to simplify their evaluation. Incorporating Kaiser's line of sight approximation for red shift space distortions allows us to write

$$\tilde{\delta}_{21}(\vec{k}) = \left( \beta + (\hat{k} \cdot \hat{r}_s)^2 \right) \tilde{\delta}_b(\vec{k}) \quad (16)$$

where we take the line of sight  $\hat{r}_s = \hat{z}$ .

We follow [16] for the definition of the  $a$ 's, and applying it to our case, for large  $l$  we define a 2-D vector  $\vec{l} = (l \cos \phi_l, l \sin \phi_l)$ , such that

$$a(\vec{l}, \chi) = \left( \sum_{m=-l}^l [(il)^{-m} \sqrt{\frac{4\pi}{2l+1} \frac{(l+m)!}{(l-m)!}} e^{im\phi_l} a_{lm}] \right) \quad (17)$$

$$\sim \int d^2\epsilon e^{(-i\vec{l} \cdot \vec{\epsilon})} \delta_{21}(\chi, \hat{x}) \quad (18)$$

so that

$$\langle a(\vec{l}, \chi) a^\dagger(\vec{l}', \chi') \rangle = \frac{2\pi}{\chi^2 \chi'^2} \delta_D^{(2)}\left(\frac{\vec{l}}{\chi} + \frac{\vec{l}'}{\chi'}\right) \int \frac{dk_3}{2\pi} \left( \beta + \frac{k_3^2}{k_3^2 + l^2/\chi^2} \right)^2 \exp[ik_3(\chi + \chi')] P_b\left(\frac{\vec{l}}{\chi}, k_3\right) \quad (19)$$

In order to get rid of the  $1/\chi^2$  dependence which prevents us from having a diagonalized correlation matrix in momentum space we will define  $b \equiv \chi^2 a(\vec{l}, \chi)$  and we consider  $b$  as a function of  $\vec{\kappa} \equiv \vec{l}/\chi$  and  $\chi$  instead of  $\vec{l}$  and  $\chi$ . We then Fourier transform in  $\chi$  and define a 3-D momentum vector  $\vec{q} = (\vec{\kappa}, k_3)$

$$\langle b(\vec{q}) b^\dagger(\vec{q}') \rangle = (2\pi)^3 \delta_D^{(3)}(\vec{q} + \vec{q}') P_{21}(\vec{q}) \quad (20)$$

$$= (2\pi)^3 \delta_D^{(3)}(\vec{q} + \vec{q}') \left( \beta + (\hat{q} \cdot \hat{z})^2 \right)^2 P_b(\vec{q}) \quad (21)$$

In doing the scaling by distance to make the signal covariance matrix diagonal, the noise covariance will become more complicated. However, the noise covariance matrix is expected to already be complicated due to non-trivial foregrounds.

### IV. FORECASTING THE ANISOTROPIES

We follow Pullen-Kamionkowski [1] and expand the anisotropic  $P_b(\vec{q})$  in terms of spherical harmonics

$$P_b(\vec{q}) = \mathcal{P}(q) \left[ 1 + \sum_{L,M} g_{L,M}(q) Y_{L,M}(\hat{q}) \right] \quad (22)$$

To estimate the constraints possible on the  $g_{L,M}$ 's, we calculate the Fisher matrix. As in [1] we will take the  $g_{L,M}(q)$  to be constant in  $q$ . We will first do the case without noise, and then we will consider the case with noise.

The Fisher matrix is

$$F = \frac{1}{2} \text{Tr} [C_{g_{L,M}} C^{-1} (C_{g_{L,M'}})^\dagger C^{-1}] \quad (23)$$

We will consider a quadrupole anisotropy, i.e.  $L=2$ . Eq. 21 is the correlation matrix  $C_{\vec{q}, \vec{q}'}$  and

$$C_{g_{L,M}} = (2\pi)^3 \delta_D^{(3)}(\vec{q} + \vec{q}') \left( \beta + (\hat{q} \cdot \hat{z})^2 \right)^2 \mathcal{P}(q) Y_{L,M}(\hat{q}) \quad (24)$$

so that

$$C_{,g_{L,M}} C^{-1} (C_{,g_{L,M}})^\dagger C^{-1} = (2\pi)^3 \delta_D^{(3)}(\vec{q} + \vec{q}') \frac{Y_{L,M}(\hat{q}) Y_{L,M'}^*(\hat{q})}{[1 + \sum_{M''} g_{L,M''} Y_{L,M''}(\hat{q})]^2} \quad (25)$$

Taking the trace of the above means setting  $q' = -q$  and integrating with measure  $\frac{d^3 q}{(2\pi)^3}$ . This leads to  $(2\pi)^3 \delta_D^{(3)}(0)$  which equals the volume of our thick tile. Thus we have

$$F_{M,M'} = \frac{1}{2} (Vol) \int \frac{d^3 q}{(2\pi)^3} \frac{Y_{L,M}(\hat{q}) Y_{L,M'}^*(\hat{q})}{[1 + \sum_{M''} g_{L,M''} Y_{L,M''}(\hat{q})]^2} \quad (26)$$

The measure  $\int d^3 q = \int_0^\infty q^2 dq \int d\Omega_{\hat{q}}$  can be regulated with the knowledge that our volume and resolution are both finite; we approximate the volume as a pixelized lattice with a total of  $N^3 \equiv N_T$  pixels. Thus

$$\frac{1}{(2\pi)^3} \int_0^\infty q^2 dq \rightarrow \frac{1}{(2\pi)^3} \frac{2\pi}{L} \sum_{j=1}^N \left(\frac{2\pi j}{L}\right)^2 \approx \left(\frac{1}{L}\right)^3 \frac{N^3}{3} = \frac{N_T}{3 Vol} \quad (27)$$

Thus we have

$$F_{M,M'} = \frac{N_T}{6} \int d\Omega_{\hat{q}} \frac{Y_{L,M}(\hat{q}) Y_{L,M'}^*(\hat{q})}{[1 + \sum_{M''} g_{L,M''} Y_{L,M''}(\hat{q})]^2} \quad (28)$$

Since we expect the  $g_{L,M''}$  to be small we evaluate the integral with  $g_{L,M''} = 0$ . By the orthonormality of the spherical harmonics we get the Fisher matrix without noise:

$$[F_{M,M'}]_{\text{noiseless}} = \frac{N_T}{6} \delta_{M,M'} \quad (29)$$

This is trivial to invert.

Now we include the beam size and instrument noise. The correlation matrix given in Eq. 21 becomes

$$C_{\vec{q},\vec{q}'} = (2\pi)^3 \delta_D^{(3)}(\vec{q} + \vec{q}') P_{21}(\vec{q}) \quad (30)$$

$$= (2\pi)^3 \delta_D^{(3)}(\vec{q} + \vec{q}') \left[ (\beta + (\hat{q} \cdot \hat{z})^2)^2 P_b(\vec{q}) \exp(-\sigma_B^2 q^2) + P_n \right] \quad (31)$$

This differs from the noiseless case by the addition of two new parameters,  $\sigma_B$  and  $P_n$ . We discuss the meaning of each in turn.

We assume a Gaussian beam characterized by a beam width  $\sigma_B$ . This beam width is related to both the radial direction (i.e. frequency resolution as given by Eq. 3) and the transverse direction angular resolution. While in general these two resolutions,  $\sigma_\chi$  for the radial and  $\sigma_T$  for the transverse, can be different, an experiment well constructed for detecting an anisotropic matter spectrum would choose them so that  $\sigma_T^2 l^2 + \sigma_\chi^2 k_3^2 = \sigma_B^2 q^2$ .

We model the instrument noise as white, uncorrelated between pixels and uniform in momentum with value  $P_n$ . We relate the noise per pixel temperature  $T_n$  to  $P_n$  through

$$(T_n / \overline{\delta T_b})^2 = \int \frac{d^3 q}{(2\pi)^3} P_n \exp(-\sigma_B^2 q^2 / (4\pi)) = \frac{P_n}{\sigma_B^3} \quad (32)$$

Here we have incorporated that cutoff as a Gaussian characterized by the beam width, but any reasonable cutoff in the momentum volume would give similar results. Varying the power-law index of the noise (to  $1/k$ , for example), affects the forecasts. Such considerations can straightforwardly be included in our analysis and we discuss them in the conclusions.

The derivative of the correlation matrix with respect to the  $g_{L=2,M}$ 's is

$$C_{,g_{L,M}} = (2\pi)^3 \delta_D^{(3)}(\vec{q} + \vec{q}') (\beta + (\hat{q} \cdot \hat{z})^2)^2 \mathcal{P}(q) \exp(-\sigma_B^2 q^2) Y_{L,M}(\hat{q}) \quad (33)$$

and the Fisher matrix becomes

$$F_{M,M'} = \frac{1}{2} (Vol) \frac{1}{(2\pi)^3} \int d^3 q \frac{Y_{L,M}(\hat{q}) Y_{L,M'}^*(\hat{q})}{\left[ 1 + \sum_{M''} g_{L,M''} Y_{L,M''}(\hat{q}) + \frac{P_n}{(\beta + (\hat{q} \cdot \hat{z})^2)^2 \mathcal{P}(q) \exp(-\sigma_B^2 q^2)} \right]^2} \quad (34)$$

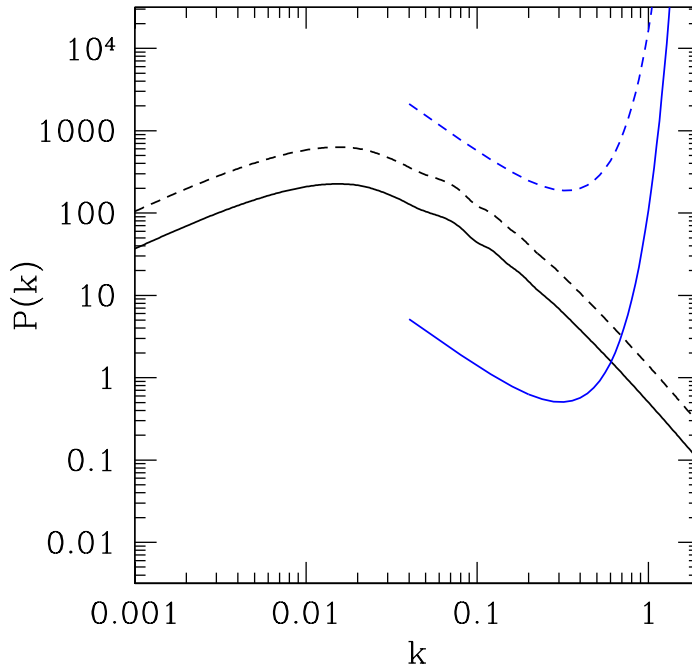


FIG. 1: Matter power spectra for  $z = 17.5$  (thick dashed) and  $z = 30$  (thick solid). The lower  $z$  curve is higher simply due to the growth of structure in linear theory. The thin blue curves show the noise per  $\ln$  interval in  $k$  assuming the experimental parameters outlined in the text. These curves include the impact of both experimental noise and the redshift evolution in the mapping between density fluctuations and temperature fluctuations. Substantial star formation at high  $z$  could lower the noise curve at  $z \sim 17.5$  by up to 4 orders of magnitude.

Again, since we expect the  $g_{L,M''}$  to be small we evaluate the integral with  $g_{L,M''} = 0$ . We are particularly interested in forecasting for the smallest redshifts before ionization, i.e.  $15 < z < 35$  which is where we can take  $\beta \approx 1.6$ . For these redshifts  $(\beta + (\hat{q} \cdot \hat{z})^2)^2$  will be between 2.56 and 6.76. We approximate our Fisher matrix by replacing  $(\hat{q} \cdot \hat{z})^2$  by  $1/2$  so that  $(\beta + (\hat{q} \cdot \hat{z})^2)^2$  is replaced by 4.41.

$$F_{M,M'} = \frac{1}{2}(\text{Vol}) \int d\Omega_{\hat{q}} Y_{L,M}(\hat{q}) Y_{L,M'}^*(\hat{q}) \frac{1}{(2\pi)^3} \int_0^\infty dq \frac{q^2}{\left[1 + \frac{P_n \exp(\sigma_B^2 q^2)}{4.41 \mathcal{P}(q)}\right]^2} \quad (35)$$

$$= \frac{1}{2} \delta_{M,M'} (\text{Vol}) \frac{1}{(2\pi)^3} \int_0^\infty dq \frac{q^2}{\left[1 + \frac{\sigma_B^3 (T_n / \delta T_b)^2 \exp(\sigma_B^2 q^2)}{4.41 \mathcal{P}(q)}\right]^2} \quad (36)$$

$$\equiv \frac{1}{2} \delta_{M,M'} (\text{Vol}) I \quad (37)$$

We evaluate numerically the integral for two cases. Case I will correspond to the Square Kilometer Array target values. Case II will correspond to the Fast Fourier transform telescope (FFTT) described in [18].

From the thermal noise per visibility as given by Morales [19] in eq. 7, we arrive at the thermal noise per pixel for the brightness temperature given by

$$T_n = \frac{\sqrt{2} T_{\text{sys}} \theta_{\text{diffraction}}}{\sqrt{B} \tau \theta_{\text{desired}}} \quad (38)$$

where  $T_{\text{sys}}$  is the system temperature,  $B$  is the bandwidth, and  $\tau$  is the total observing time.  $\theta_{\text{diffraction}}$  is the diffraction limited resolution  $\lambda_{21}(1+z)/\sqrt{A_e}$  ( $A_e$  is the effective antenna area) and  $\theta_{\text{desired}}$  is the 1 arcminute resolution we desire. The angular resolution is assumed to be tuned by a dilution of the array from being fully compact by a simple scaling

of all baseline positions by a fixed amount. The system temperature is given by ARCADE 2 [20] as

$$T_{\text{sys}} = 1.26 \text{ K} \left( (1+z) \frac{1 \text{ GHz}}{\nu_{21}} \right)^{2.6} \quad (39)$$

Putting this together we arrive at an expression for the noise as a function of redshift assuming that an array is simply scaled to maintain constant angular resolution:

$$T_n = \frac{12 \text{ mK}}{\sqrt{(\tau/10^4 \text{ hr})(A_e/\text{km}^2)}} \left( \frac{1+z}{21} \right)^{3.85} \left[ \frac{\sqrt{1+z}}{\sqrt{1+z-1}} \right]^{1/2} \quad (40)$$

The noise is a steeply rising function of redshift, but the signal is also a strong function of redshift in the dark ages just before reionization. For example, if star formation has not started in earnest by  $z \sim 17$ , we can see from the table below that the mean 21cm brightness temperature at  $z = 30$  is 30 times larger, while the noise is higher by only a factor of 8. The growth of fluctuations boosts the lower  $z$  signal by a factor of 1.7, but that still leaves more than a factor of 2 higher sensitivity at  $z \sim 30$  compared to  $z \sim 17$ .

For both our cases we will consider 10 000 hours of total observing time. For case I, the SKA, we consider a line of sight depth of redshift  $z = 15$  to 20, i.e. 374 Mpc/h. The effective antenna area is 1 sq km. This gives an average noise per pixel of about  $T_n = 8$  mK. The total area of sky observed is taken to be 250 degrees.

For case II, the FTTT (or ‘‘Omniscop’’), we consider a line of sight depth of  $z = 25$  to 35, i.e 346 Mpc/h. The effective antenna area is 100 sq km, the limit at which earth curvature could be a problem [18]. This gives an average noise per pixel of about  $T_n = 6$  mK. The total area of sky observed is taken to be 3000 degrees, to account for edge effects not allowing a full 1/2 sky.

These two cases correspond to a central redshift values of  $z = 17.5$  and  $z = 30$  respectively. Because of our finite box size we impose a lower limit in the  $dq$  integration corresponding to  $2\pi$  divided by the smallest dimension of the box, which is the line of sight direction. We have for the  $z \in [15, 20]$  and  $z \in [25, 30]$  a lower momentum cutoff of 0.0168 h/Mpc and 0.0181 h/Mpc, respectively. In the numerical evaluation of the integral we have checked that replacing this lower momentum cutoff by zero does not significantly affect the result.

We take our beam width  $\sigma_B$  to correspond to the length scale of 1 arcminute at the comoving distance of interest. For  $z=17.5$  and  $z=30$ , the comoving distance is 9020 Mpc/h and 9650 Mpc/h, respectively, and the beam width is 2.63 Mpc/h and 2.81 Mpc/h, respectively.

We use the linear matter power spectrum as provided in the LAMBDA CAMB Web Interface Toolbox [17]. The power spectra can be seen in Figure 1 for the different redshift choices, along with the noise curves for the assumed experimental parameters. For the high redshift case, the signal to noise is much higher for two reasons: the assumed noise level is slightly smaller in power (the increased noise at higher  $z$  is assumed to be more than offset by a larger collecting area), and the expected cosmological mean signal (in mK) is substantially larger, leading to a significantly stronger constraint on the matter power spectrum for the nominal higher redshift experiment.

We summarize our results for the two cases in the following table.

Case	$z$	$\overline{\delta T_b}$ [mK]	$T_n/\text{pixel}$ [mK]	beam width [Mpc/h]	angular size [sq. deg.]	vol [(Gpc/h) <sup>3</sup> ]	I [(h/Mpc) <sup>3</sup> ]	$\sigma[g_{2M}] = F^{-1/2}$
I	15-20	-0.150	8	2.63	250	2.32	$4.11 \times 10^{-11}$	4.6
II	25-35	-4.42	6	2.81	3000	29.45	$2.04 \times 10^{-6}$	0.006

## V. CONCLUSIONS AND DISCUSSION

The results in the above table mean that 21 cm surveys should be able to constrain the values of  $g_{2M}$  to about  $1/\sqrt{0.0476} = 4.6$  for case I and  $1/\sqrt{30000} = 0.006$  for case II. If instead of white noise, we allow for a  $P_n(q) \sim 1/q$ , then the constraints on the values of  $g_{2M}$  are 43 and 0.03 for cases I and case II, respectively.

While the noise per mode is quite high, the large volume allows a huge number of modes to be measured. For example, 1 (Gpc/h)<sup>3</sup> of volume provides (in principle) more than  $3 \times 10^7$  measurements with  $\sim$  Mpc/h resolution. Even with such a large number of samples, we see that this is a challenging measurement with planned upcoming experiments such as SKA; to accurately measure this signal with 21cm experiments will necessitate deeper maps, to push the signal to noise per mode high enough to reach the sample variance limit.

One way to increase the signal to noise is to measure the signal at higher redshift, where the pre-reionization hydrogen spin temperature difference from the CMB is larger. At  $z \sim 28$  the mean temperature difference is 30x larger than at  $z \sim 17$ , in the absence of reionization effects, while the sky noise is higher by less than a factor of 10. It has been suggested that reionization could boost the  $z \sim 17$  signal by up to two orders of magnitude [9]; if the

reionization process doesn't compromise the signal of interest, this would allow SKA to have a measurement of the anisotropy to better than ten percent.

The promise of future 21cm experiments is evident from the large signal to noise that is possible from a sufficiently sensitive experiment. This is in contrast to CMB experiments, where cosmological information is now largely limited by the finite number of modes that can be measured within the boundaries imposed by causality. For future 21cm experiments, limits will be set by experimental capabilities, but precise measurements at high redshift (i.e., lower frequencies) will allow powerful constraints on fundamental physics.

### Acknowledgments

This work is supported by the FQRNT Programme de recherche pour les enseignants de coll ge, the Canadian Institute for Advanced Research, the NSERC Discovery program, and the Canada Research Chairs program.

- 
- [1] A. R. Pullen and M. Kamionkowski, Phys. Rev. D **76**, 103529 (2007) [arXiv:0709.1144 [astro-ph]].
  - [2] L. Ackerman, S. M. Carroll and M. B. Wise, Phys. Rev. D **75**, 083502 (2007) [Erratum-ibid. D **80**, 069901 (2009)] [arXiv:astro-ph/0701357].
  - [3] [Bennett et al.(2010)]2010arXiv1001.4758B Bennett, C. L., et al. 2010, arXiv:1001.4758
  - [4] N. E. Groeneboom, L. Ackerman, I. K. Wehus and H. K. Eriksen, arXiv:0911.0150 [astro-ph.CO].
  - [5] [Planck Collaboration et al.(2011)]2011arXiv1101.2022P Planck Collaboration, et al. 2011, arXiv:1101.2022
  - [6] Pullen, A. R., & Hirata, C. M. 2010, JCAP, 5, 27
  - [7] S. Furlanetto, S. P. Oh and F. Briggs, Phys. Rept. **433**, 181 (2006) [arXiv:astro-ph/0608032].
  - [8] [Dewdney et al.(2009)]2009IEEEP..97.1482D Dewdney, P. E., Hall, P. J., Schilizzi, R. T., & Lazio, T. J. L. W. 2009, IEEE Proceedings, 97, 1482
  - [9] Furlanetto, S. R. 2006, MNRAS, 371, 867
  - [10] Furlanetto, S. R., et al. 2009, astro2010: The Astronomy and Astrophysics Decadal Survey, 2010, 82
  - [11] B. Zygelman, Astrophys. J. 622 (2005) 13561362. Zygelman B., 2005, ApJ, 622, 1356
  - [12] S. Furlanetto and M. Furlanetto, Mon. Not. Roy. Astron. Soc. **374**, 547 (2007) [arXiv:astro-ph/0608067].
  - [13] S. Bharadwaj and S. S. Ali, Mon. Not. Roy. Astron. Soc. **352**, 142 (2004) [arXiv:astro-ph/0401206].
  - [14] N. Kaiser, Mon. Not. Roy. Astron. Soc. **227**, 1 (1987).
  - [15] O. Lahav, P. B. Lilje, J. R. Primack and M. J. Rees, Mon. Not. Roy. Astron. Soc. **251**, 128 (1991).
  - [16] M. J. White, J. E. Carlstrom and M. Dragovan, W. L. Holzappel Astrophys. J. **514**, 12 (1999) [arXiv:astro-ph/9712195].
  - [17] LAMBDA CAMB Web Interface Toolbox [http://lambda.gsfc.nasa.gov/toolbox/tb\\_camb\\_form.cfm](http://lambda.gsfc.nasa.gov/toolbox/tb_camb_form.cfm).
  - [18] M. Tegmark and M. Zaldarriaga, Phys. Rev. D **79**, 083530 (2009) [arXiv:0805.4414 [astro-ph]].
  - [19] M. F. Morales, Astrophys. J. **619**, 678 (2005) [arXiv:astro-ph/0406662].
  - [20] D. J. Fixsen *et al.*, arXiv:0901.0555 [astro-ph.CO].